ISSN 0915-633X

NATIONAL INSTITUTE FOR FUSION SCIENCE

Formation of Presheath and Current-Free Double Layer in a Two-Electron-Temperature Plasma

K. Sato and F. Miyawaki

(Received – Jan. 13, 1992)

NIFS-132 Feb. 1992

RESEARCH REPORT
NIFS Series

NAGOYA, JAPAN

Formation of Presheath and Current-Free Double Layer in a Two-Electron-Temperature Plasma

Kunihiro Sato and Fujio Miyawaki

Department of Electrical Engineering,

Himeji Institute of Technology,

Himeji 671-22, Japan

ABSTRACT

Development of the steady-state potential in a two-temperature-electron plasma in contact with the wall is investigated analytically. It is shown that if the hot- to cold electron temperature ratio is greater than ten, the potential drop in the presheath, which is allowed to have either a small value characterized by the cold electrons or a large value by the hot electrons, discontinuously changes at a critical value for the hot- to total electron density ratio. It is also found that the monotonically decreasing potential structure which consists of the first presheath, a current-free double layer, the second presheath, and the sheath can be steadily formed in a lower range of the hot- to total electron density ratio around the critical value. The current-free double layer is set up due to existence of the two electron species and cold ions generated by ionization so as to connect two presheath potentials at different levels.

Keywords; presheath, current-free double layer, two-temperature-electron plasma, potential formation, energetic electrons, plasma equation

I. INTRODUCTION

A plasma with energetic electrons or a two-electron-population plasma is produced in various laboratory devices. In tokamak experiments using ion cyclotron frequency heating, lower-hybrid wave heating, and rf current-drive, non-thermal electrons appear in scrape-off layer due to strong rf fields[1,2]. In the tandem mirror, during strong electron cyclotron resonance heating, the electron distribution composed of two Maxwellians at different temperatures is observed in the open end region in front of end plates[3]. In the negative ion source, fast primary electrons for excitation of hydrogen molecules and slow plasma electrons for production of negative ions are required in order to improve volume production of negative hydrogen ions[4].

Two-isothermal species of electrons have also been observed in the expanding corona of a plasma heated by a laser[5]. The expansion of such a plasma and the development of a potential double layer, called a rarefaction shock, have been investigated theoretically, and general conditions under which rarefaction shocks can exist was derived[6,7]. Recently, a laboratory experiment of the expansion of a two-electron-population plasma has been carried out by Hairapetian et al.[8]. They have also observed a stationary, current-free, potential double layer which is formed due to self-consistent separation of the two electron species in the same devices[9].

The appearance of energetic electrons is expected to have a remarkable effect on potential formation in the plasma because the potential formation is closely associated with the electrons distribution. While there has been considerable theoretical activity in the problem of potential formation in a plasma bounded by the wall since the kinetic

analysis in the context of discharge plasma was done by Tonks and Langmuir[10–13], we know of few attempt to verify the characteristics of the potential formed in two-electron-population plasmas.

In this paper, we theoretically investigate the steady-state potential formation in a two-electron-temperature plasma to show possibility of steady-state potential formation, to clarify the potential structure, and to evaluate the potential drop in such a plasma. The ions are assumed to be generated by ionization of neutral atoms without thermal motion, and the electrons are assumed to have two Maxwellian distributions at different temperatures, T_h and T_c. We analytically solve the plasma equation, and check whether the analytic solution satisfies a condition for the formation of a stable sheath potential. Results calculated from the analytic solution show that the potential drop in the presheath has either a small value characterized by the cold electrons or a large one by the hot electrons if the temperature ratio T_h/T_c is greater than 10. There is a critical value for the hot- to total electron density ratio at which the potential drop of presheath discontinuously increase from the low level to the high one as the density ratio increases.

We also find that the steady-state monotonically decreasing potential which consists of the first presheath, a current-free double layer, the second presheath, and the sheath just in front of the wall can be set up in a lower range of the hot- to total electron density ratio around the critical value. The present double layer builds up in the plasma without plasma current, while most double layers observed in experiments[14] or theoretically investigated[15] require the presence of a plasma current. The double layer structure is sustained by self-consistent separation of the two electron species and generation of ions

at the two presheathes. The formation mechanism is similar to that of the double layer experimentally observed by Hairapetian et al.[9].

In Sec. II, we present the solution of the plasma equation, and briefly discuss a condition for the formation of a stable sheath potential. The formation of the double layer and the solution of the plasma equation for the second presheath is described in Sec. III. Results calculated from the analytic solutions are illustrated and discussed in Sec. IV, and the conclusions are summarized in Sec. V.

II. SOLUTION OF THE PLASMA EQUATION

A collisionless plasma is assumed in a one-dimensional planar geometry with walls at $x = \pm L$, which are perfectly absorbing and electrically floating. The electrostatic potential $\phi(x)$, which is defined to be zero at $x = 0$, is expected to be monotonically decreasing for $x > 0$ as shown Fig. 1. The ion density $n_i(x)$ at some point x is described by a kinetic equation

$$n_i(x) = < \sigma v > n_0 n_n \int_0^x dx' \, h(x') \left[2q \left\{\phi(x') - \phi(x)\right\} / M\right]^{-1/2} \quad , \tag{1}$$

where q and M are the charge and mass of the ion, $< \sigma v >$ is the ionization rate coefficient, n_0 is the electron density at $x = 0$, and n_n is the neutral atom density. The function $h(x)$ expresses the spatial variation of the ionization rate. It is assumed that the initial thermal velocity of the ion is negligibly small. For electrons the distribution composed of two Maxwellians at different temperatures is adopted to give the electron density

$$n_e(x) = n_{c0}\exp[e\phi(x)/kT_c] + n_{h0}\exp[e\phi(x)/kT_h] \quad , \tag{2}$$

where n_{c0} and n_{h0} are the cold and hot electron particle densities at $x = 0$, and T_c and T_h are the cold and hot electron temperatures. Substituting Eqs. (1) and (2) into Poisson's equation, we obtain the integrodifferential equation

$$\lambda_{d0}^2 \frac{e}{kT_c}\frac{d^2\phi}{dx^2} = \frac{n_{c0}}{n_0}\exp[e\phi(x)/kT_c] + \frac{n_{h0}}{n_0}\exp[e\phi(x)/kT_h] - < \sigma v > n_n \left(\frac{Mq}{2e}\right)^{1/2} \int_0^x dx' h(x')[\phi(x') - \phi(x)]^{-1/2} \quad , \tag{3}$$

where λ_{d0} is the Debye length at $x = 0$ defined by $\lambda_{d0}^2 = \epsilon_0 kT_c/n_0 e^2$.

The plasma equation, which describes the potential distribution in the plasma expect the sheath, is obtained by neglecting the second derivative term of Eq. (3). With the introduction of the dimensionless variables

$$s = x/L\,, \quad Z = q/e\,, \quad \alpha = n_{h0}/n_0\,, \quad \tau = T_h/T_c\,, \quad \Psi(s) = -e\phi(x)/kT_c\,,$$

the plasma equation is written in the form

$$(1-\alpha)\exp(-\Psi) + \alpha\exp(-\Psi/\tau) = A\int_0^\Psi d\Psi' \frac{ds'}{d\Psi'}\frac{h(\Psi')}{(\Psi - \Psi')^{1/2}} \quad , \tag{4}$$

where

$$A = < \sigma v > n_n \left(\frac{ZM}{2kT_c}\right)^{1/2} L$$

and $\Psi' = \Psi(s')$. Equation (4) is Abel's integral equation and its solution is[16]

$$Ah(\Psi)\frac{ds}{d\Psi} = \frac{1}{\pi}\frac{d}{d\Psi}\int_0^\Psi d\Psi' \frac{(1-\alpha)\exp(-\Psi') + \alpha\exp(-\Psi'/\tau)}{(\Psi - \Psi')^{1/2}} \quad . \tag{5}$$

The differentiation on the right-hand side in Eq. (5) can be carried out to give

$$\frac{ds}{d\Psi} =$$

$$\frac{1}{\pi A h(\Psi)} \left[\frac{1}{\sqrt{\Psi}} - 2(1-\alpha)\exp(-\Psi) D\left(\sqrt{\Psi}\right) - 2\frac{\alpha}{\sqrt{\tau}} \exp(-\Psi/\tau) D\left(\sqrt{\Psi/\tau}\right) \right]$$

$$, \quad 0 \leq \Psi \leq \Psi_1 \ , \tag{6}$$

where $D(x)$ is the Dawson function and Ψ_1 is the potential at the plasma-sheath boundary. In the absence of a boundary condition there is always a solution to the plasma equation for any value of Ψ_1, but the solution satisfies the general Bohm criterion at the boundary only if $ds/d\Psi = 0$ at $\Psi = \Psi_1$[17]. With the aid of this boundary condition, the value of Ψ_1 is determined from the equation

$$\frac{1}{2\sqrt{\Psi_1}} = (1-\alpha)\exp(-\Psi_1) D\left(\sqrt{\Psi_1}\right) + \frac{\alpha}{\sqrt{\tau}} \exp(-\Psi_1/\tau) D\left(\sqrt{\Psi_1/\tau}\right) \ . \tag{7}$$

Integration of Eq. (6) give the function $s(\Psi)$ from which the profile of the potential in the plasma up to the edge of the sheath, the so-called presheath, is determined ;

$$s(\Psi) = \int_0^{\Psi} d\Psi' \frac{ds'}{d\Psi'} \left(\int_0^{\Psi_1} d\Psi' \frac{ds'}{d\Psi'} \right)^{-1} \ . \tag{8}$$

It is seen from Eqs. (6)-(8) that while the profile of the potential depends on the shape of $h(\Psi)$, the potential at the boundary is independent of it. We can calculate the profile of the presheath potential from Eq. (8) once the function $h(\Psi)$ is specified.

The wall potential Ψ_w is determined from the requirement that the electron flux and the ion flux must be equal at the wall. Since the particle number of ions generated in the sheath can be neglected in the limit as $\lambda_{d0}/L \to 0$, the ion flux is evaluated by integrating the particle source in the plasma as

$$Z\Gamma_i = n_0 \left(\frac{2ZkT_c}{M}\right)^{1/2} A \int_0^{\Psi_1} d\Psi' \frac{ds'}{d\Psi'} h(\Psi') \ , \tag{9}$$

which is independent of the shape of $h(\Psi)$. The integration in Eq. (9) can be carried out using Eq. (6). The electron flux of the two-temperature electron is expressed by

$$\Gamma_e = n_0 \left(\frac{kT_c}{2\pi m}\right)^{1/2} \left[(1-\alpha)\exp(-\Psi_w) + \alpha\sqrt{\tau}\exp(-\Psi_w/\tau)\right] \ , \tag{10}$$

and then, we obtain the equation from which the value of Ψ_w is determined as

$$(1-\alpha)\exp(-\Psi_w) + \alpha\sqrt{\tau}\exp(-\Psi_w/\tau) = \left(\frac{16mZ}{\pi M}\right)^{1/2} \left[(1-\alpha)\exp(-\Psi_1) D\left(\sqrt{\Psi_1}\right) + \alpha\sqrt{\tau}\exp(-\Psi_1/\tau) D\left(\sqrt{\Psi_1/\tau}\right)\right] \ . \tag{11}$$

We now derive the sheath equation and briefly discuss a condition for the formation of the sheath potentials. Multiplying by $d\Psi/ds$ and integrating Poisson's equation, we obtain the equation which described the sheath potential as follow ;

$$\frac{1}{2}\left(\frac{\lambda_{d0}}{L}\right)^2 \left(\frac{d\Psi}{ds}\right)^2 = \int_{\Psi_1}^{\Psi} d\Psi' \left[Zn_i(\Psi') - n_e(\Psi')\right]/n_0 \ . \tag{12}$$

Since the left band side of Eq. (12) is positive, the inequality

$$\int_{\Psi_1}^{\Psi} d\Psi' (Zn_i - n_e) \geq 0 \tag{13}$$

must hold over the range $\Psi_1 < \Psi \leq \Psi_w$, which is the condition for the formation of a stable sheath potential. For a maxwellian distribution of electron, the inequality (13) always holds true once the generalized Bohm criterion is satisfied at $\Psi = \Psi_1$ because of rapid decrease of the electron particle density with increase of the potential. But, for

electron which has a high energy component, the inequality (13) doesn't always hold even if the generalized Bohm criterion is satisfied at the boundary. The ion density in the sheath is obtain from

$$n_i(\Psi) = \frac{A}{Z}\int_0^{\Psi_1} d\Psi' \frac{ds'}{d\Psi'} \frac{h(\Psi')}{(\Psi - \Psi')^{1/2}} \tag{14}$$

by using the solution of the plasma equation, Eq. (6). Carrying out some integration, we can write the inequality (13) as

$$\begin{aligned} &\Psi - \Psi_1 - \frac{2}{\pi}\int_{\Psi_1}^{\Psi} d\Psi' (\Psi/\Psi' - 1)^{1/2} - \frac{4}{\pi}\int_0^{\Psi_1} d\Psi' \left[(\Psi - \Psi')^{1/2} - (\Psi_1 - \Psi')^{1/2}\right] \\ &\quad \times \left[(1-\alpha)\exp(-\Psi') D\left(\sqrt{\Psi'}\right) + \frac{\alpha}{\sqrt{\tau}} \exp(-\Psi'/\tau) D\left(\sqrt{\Psi'/\tau}\right)\right] \\ &\quad -(1-\alpha)\left[\exp(-\Psi_1) - \exp(-\Psi)\right] - \alpha\tau\left[\exp(-\Psi_1/\tau) - \exp(-\Psi/\tau)\right] \\ &\quad \geq 0 \ . \end{aligned} \tag{15}$$

If this condition is not satisfied over the range $\Psi_1 < \Psi \leq \Psi_w$, there is not a nonoscillatory solution which can reach to the potential Ψ_w. In this case, we can find another monotonically decreasing potential structure which consists of the first presheath, a double layer, the second presheath, and a sheath as described in the next section.

III. CURRENT-FREE DOUBLE LAYER AND THE SECOND PRESHEATH

When a sign of the integral in Eq. (12) changes from positive to negative as the potential Ψ increases, we can get a monotonically decreasing solution of Poisson's equation which can reach the wall potential by introducing formation of a double layer and the second presheath downstream from the first presheath. A double layer is a localized electrostatic potential structure created by two equal but opposite space-charge layers. The potential of the double layer placed to the first presheath is calculated from Eq. (12), and the edge potential Ψ_D is determined from

$$\int_{\Psi_1}^{\Psi_D} d\Psi'(Zn_i - n_e) = 0 \ . \tag{16}$$

This double layer is surrounded by the first and second presheathes, and is sustained by the ionization of neutral atoms in the presheath regions. Appearance of the cold ion in the second presheath enable the steady-state double layer to be set up in the plasma.

The thickness of a double layer is generally from a few ten times to several hundred times of the Debye length, then the particle source inside the double layer can be neglected in the limit as $\lambda_{d0}/L \to 0$. Neglecting the particle source in the double layer, we can describe the ion density in the second presheath by the equation

$$Zn_i(s) = An_0 \left[\int_0^{\Psi_1} d\Psi' \frac{ds'}{d\Psi'} \frac{h(\Psi')}{(\Psi - \Psi')^{1/2}} + \int_{\Psi_D}^{\Psi} d\Psi' \frac{ds'}{d\Psi'} \frac{h(\Psi')}{(\Psi - \Psi')^{1/2}} \right] \ , \tag{17}$$

where the first term on the right hand side is the particle density of ions produced in the first presheath and the second one is that produced in the second presheath. Equalizing

the ion density to the electron density and introducing the transformation $\xi = \Psi - \Psi_D$, the plasma equation of the second presheath is written as

$$(1-\alpha)\exp\left[-(\Psi_D+\xi)\right] + \alpha\exp\left[-(\Psi_D+\xi)/\tau\right]$$
$$= A\int_0^{\Psi_1} d\Psi' \frac{ds'}{d\Psi'}\frac{h(\Psi')}{(\Psi_D+\xi-\Psi')^{1/2}} + A\int_0^{\xi} d\xi' \frac{ds'}{d\xi'}\frac{h(\Psi_D+\xi')}{(\xi-\xi')^{1/2}} \ . \qquad (18)$$

Since the first integral on the right hand side is a function of ξ, Equation (18) becomes Abel's integral equation and its solution is

$$Ah(\Psi_D+\xi)\frac{ds}{d\xi} = \frac{1}{\pi}\frac{d}{d\xi}\int_0^{\xi}\frac{d\xi'}{(\xi-\xi')^{1/2}}\left\{(1-\alpha)\exp\left[-(\Psi_D+\xi')\right]\right.$$
$$\left.+\alpha\exp\left[-(\Psi_D+\xi')/\tau\right] - A\int_0^{\Psi_1} d\Psi' \frac{ds'}{d\Psi'}\frac{h(\Psi')}{(\Psi_D+\xi'-\Psi')^{1/2}}\right\} \ . \qquad (19)$$

Putting Eq. (6) into Eq.(19) and carrying out some integration and derivation give the result

$$\frac{ds}{d\Psi} =$$
$$\frac{1}{\pi A h(\Psi)}\left\{(1-\alpha)\left[(\Psi-\Psi_D)^{-1/2}\exp(-\Psi_D) - 2\exp(-\Psi)D\left(\sqrt{\Psi-\Psi_D}\right)\right]\right.$$
$$+\alpha\left[(\Psi-\Psi_D)^{-1/2}\exp(-\Psi_D/\tau) - \frac{2}{\sqrt{\tau}}\exp(-\Psi/\tau)D\left(\sqrt{(\Psi-\Psi_D)/\tau}\right)\right]$$
$$-\frac{1}{\pi}\int_0^{\Psi_1}\frac{d\Psi'}{\Psi-\Psi'}\left(\frac{\Psi_D-\Psi'}{\Psi-\Psi_D}\right)^{1/2}\left[\frac{1}{\sqrt{\Psi'}} - 2(1-\alpha)\exp(-\Psi')D\left(\sqrt{\Psi'}\right)\right.$$
$$\left.\left.-2\frac{\alpha}{\sqrt{\tau}}\exp(-\Psi'/\tau)D\left(\sqrt{\Psi'/\tau}\right)\right]\right\} \ , \quad \Psi_D \le \Psi \le \Psi_2 \ . \qquad (20)$$

The potential at the edge of the second presheath, Ψ_2, is determined from the boundary condition, $ds/d\Psi = 0$.

In the limit as $\lambda_{d0}/L \to 0$, the position of the double layer is determined by using the solution of the plasma equation. The position of the double layer, s_D, is given by

$$s_D = \int_0^{\Psi_1} d\Psi' \frac{ds'}{d\Psi'} \tag{21}$$

and the position of the wall by

$$1 = s_D + \int_{\Psi_D}^{\Psi_2} d\Psi' \frac{ds'}{d\Psi'} \ , \tag{22}$$

and then s_D is expressed as

$$s_D = \left[1 + \int_{\Psi_D}^{\Psi_2} d\Psi' \frac{ds'}{d\Psi'} \left(\int_0^{\Psi_1} d\Psi' \frac{ds'}{d\Psi'} \right)^{-1} \right]^{-1} \ . \tag{23}$$

It is seen from Eq. (23) that the position s_D depends on the spatial profile of the particle source because the integrand ds/Ψ varies inversely as $h(s)$, while the potentials Ψ_1, Ψ_2, Ψ_D, and Ψ_w are independent of $h(s)$. The potential profile in the first and second presheathes is found from the integral

$$s(\Psi) = s_D \int_0^{\Psi} d\Psi' \frac{ds'}{d\Psi'} \left(\int_0^{\Psi_1} d\Psi' \frac{ds'}{d\Psi'} \right)^{-1} \ , \quad 0 < s < s_D \tag{24}$$

and

$$s(\Psi) = s_D + (1 - s_D) \int_{\Psi_D}^{\Psi} d\Psi' \frac{ds'}{d\Psi'} \left(\int_{\Psi_D}^{\Psi_2} d\Psi' \frac{ds'}{d\Psi'} \right)^{-1} \ , \quad s_D < s < 1 \tag{25}$$

which depends on the spatial profile of the particle source.

Since the cold electrons are reflected by the double layer potential, the electron distribution function at the second presheath is close to a Maxwellian with the temperature T_h. In this case, a nonoscillatory stable sheath potential is always formed just in front of the wall once the generalized Bohm criterion is satisfied at the edge of the second presheath. The ion flux is evaluated by integrating the particle source as

$$Z\Gamma_i = n_0 \left(\frac{2ZkT_c}{M}\right)^{1/2} A \left[\int_0^{\Psi_1} d\Psi' \frac{ds'}{d\Psi'} h(\Psi') + \int_{\Psi_D}^{\Psi_2} \frac{ds'}{d\Psi'} h(\Psi')\right] \quad . \tag{26}$$

Carrying out the integration in Eq. (26) and equating the electron and ion fluxes, we obtain the equation to determine the wall potential as

$$\begin{aligned}
&(1-\alpha)\exp(-\Psi_w) + \alpha\sqrt{\tau}\exp(-\Psi_w/\tau) \\
&\quad = \left(\frac{16mZ}{\pi M}\right)^{1/2} \Bigg\{ (1-\alpha)\left[\exp(-\Psi_1) D\left(\sqrt{\Psi_1}\right) + \exp(-\Psi_2) D\left(\sqrt{\Psi_2 - \Psi_D}\right)\right] \\
&\qquad + \alpha\sqrt{\tau}\left[\exp(-\Psi_1/\tau) D\left(\sqrt{\Psi_1/\tau}\right) + \exp(-\Psi_2/\tau) D\left(\sqrt{(\Psi_2 - \Psi_D)/\tau}\right)\right] \\
&\qquad - \frac{1}{\pi}\int_0^{\Psi_1} d\Psi' \tan^{-1}\left[\left(\frac{\Psi_2 - \Psi_D}{\Psi_D - \Psi'}\right)^{1/2}\right] \left[\frac{1}{\sqrt{\Psi'}} - 2(1-\alpha)\exp(-\Psi') D\left(\sqrt{\Psi'}\right)\right. \\
&\qquad \left. - 2\frac{\alpha}{\sqrt{\tau}}\exp(-\Psi'/\tau) D\left(\sqrt{\Psi'/\tau}\right)\right] \Bigg\} \quad .
\end{aligned} \tag{27}$$

The potential Ψ_w weakly depends on Zm/M, while the potentials Ψ_1, Ψ_D, and Ψ_2 are independent of it.

Using the solution, we can also calculate the ion distribution function explicitly. To express the distribution function, we use the normalized quantities and the normalized velocity, $V = v/(2kT_c/M)^{1/2}$. An ion generated at a point $s' \leq s$ has a velocity of

$$V = \{Z[\Psi(s) - \Psi(s')]\}^{1/2} \quad . \tag{28}$$

If $f(V)dV$ is the number of ions at having velocities in the range V to $V + dV$, it follows that

$$f(V)dV = An_0 h(s')ds'/V \quad , \tag{29}$$

where the right hand is the number of ions generated per second between s' and $s'+ds'$. From Equations (28) and (29), therefore, the distribution function at a point $s \geq s'$, normalized to n_0, is given by

$$\frac{f(V)}{n_0} = \frac{2A}{Z^{3/2}} h(s') \frac{ds'}{d\Psi'} \ , \tag{30}$$

which is independent of the spatial profile of the particle source. Substituting Eqs. (5) and (20), we can express the distribution function at the edge of the second presheath in the form ;

$$\begin{aligned}\frac{f_2(V)}{n_0} = \frac{2}{\pi Z^{3/2}} \Bigg\{ & (1-\alpha) \left[(\Psi' - \Psi_D)^{-1/2} \exp(-\Psi_D) - 2\exp(-\Psi') D\left(\sqrt{\Psi' - \Psi_D}\right) \right] \\ & + \alpha \left[(\Psi' - \Psi_D)^{-1/2} \exp(-\Psi_D/\tau) - \frac{2}{\sqrt{\tau}} \exp(\Psi'/\tau) D\left(\sqrt{(\Psi' - \Psi_D)/\tau}\right) \right] \\ & - \frac{1}{\pi} \int_0^{\Psi_1} \frac{d\Psi''}{\Psi' - \Psi''} \left(\frac{\Psi_D - \Psi''}{\Psi' - \Psi_D} \right)^{1/2} \left[\frac{1}{\sqrt{\Psi''}} - 2(1-\alpha)\exp(-\Psi'') D\left(\sqrt{\Psi''}\right) \right. \\ & \left. - 2\frac{\alpha}{\sqrt{\tau}} \exp(-\Psi''/\tau) D\left(\sqrt{-\Psi''/\tau}\right) \right] \Bigg\} \\ & , \ 0 < V < [Z(\Psi_2 - \Psi_D)]^{1/2} \ , \end{aligned} \tag{31a}$$

and

$$\begin{aligned}\frac{f_2(V)}{n_0} = \frac{2}{\pi Z^{3/2}} \left[\frac{1}{\sqrt{\Psi'}} - 2(1-\alpha)\exp(-\Psi') D\left(\sqrt{\Psi'}\right) - 2\frac{\alpha}{\sqrt{\tau}} \exp(-\Psi'/\tau) D\left(\sqrt{\Psi'/\tau}\right) \right] \\ , \ [Z(\Psi_2 - \Psi_1)]^{1/2} < V < (Z\Psi_2)^{1/2} \ , \end{aligned} \tag{31b}$$

where $\Psi' = \Psi_2 - V^2/Z$. The ion distribution is separated into two parts due to the formation of the double layer. The ions produced in the first presheath are accelerated by the double layer to form a high-energy beam expressed by Eq. (31b). In the same manner, we can also get the expression of the heat flux using the solution of the plasma equation.

IV. RESULTS AND DISCUSSION

The plasma-sheath boundary potential is obtained by finding the value of Ψ_1 that satisfied Eq. (7) for a particular value of the temperature ratio τ and the density ratio n_{h0}/n_0. The results of the potential as a function of the density ratio n_{h0}/n_0 are shown in Fig. 2. When the temperature ratio τ is smaller than 10, Equation (7) has a single root and then the potential Ψ_1 is continually changing from 0.85 to 0.85 τ as the density ratio increases. When the value of τ is larger than 10, however, Equation (7) has three roots in some range of n_{h0}/n_0. In this case, we must choose the smallest one as the boundary potential to get physically meaningful potential profile in the presheath because the derivative $ds/d\Psi$, the reciprocal of the normalized electric field, must be a single value at any point in the real space. Following this fact we can see that the potential Ψ_1 discontinuously changes from a value of order of 1 to one of order of τ at some value of n_{h0}/n_0 when $\tau > 10$. It is noted that the condition $\tau > 10$ agrees well with a necessary condition given by $\tau > 5+\sqrt{24}$ for rarefaction shocks to exist in a laser-plasma corona[6,7].

It is also noted that there is the range of n_{h0}/n_0 where the condition for sheath formation described by the inequality (15) is not satisfied. In this range, which is indicated by using broken lines in Fig. 2, a monotonically decreasing potential structure composed by the first presheath, a current-free double layer, the second presheath, and the sheath builds up in the plasma in stead of the usual potential structure composed by the presheath and the sheath. The potential at the edge of the first and second presheathes, Ψ_1 and Ψ_2, are determined from the boundary condition, $ds/d\Psi = 0$, and that of the double layer, Ψ_D, is calculated from Eq. (16). Results for $\tau = 20$ shown in Fig. 3(a) and

for $\tau = 50$ in Fig. 3(b) show that the potential drop in the first presheath is of the order of the cold electron temperature and that in the second presheath of the order of the hot electron temperature. The potential at the edge of the double layer, Ψ_D, is continuously changing from Ψ_2 to Ψ_1 as the density ratio increases. The wall potential calculated from Eqs. (11) and (27) for a hydrogen plasma is shown in Fig. 4. The wall potential, which is mainly dominated by the hot electrons, is continuously changing regardless of discontinuous change of the presheath potential and the potential structure.

The potential profile of the presheath which ends to the wall through the sheath is plotted in Fig. 5 for various values of n_{h0}/n_0. Here the spatial profile of the particle source is assumed to be of the form $h(s) = n(s)/n_0$, so that the ionization rate is proportional to the electron density. Symbols a, f, and e represent the results for the points in Fig. 2. It is noted that between point a and b the potential drop in the presheath drastically increases as n_{h0}/n_0 increases.

The profile of the presheath potential for various value of the density ratio n_{h0}/n_0 in the range where the double layer and the second presheath build up at downstream of the first presheath is calculated from Eqs. (24) and (25). Results are shown Fig. 6, where b, c, and d represent the results for the points in Fig. 3(a). The potential drop at the current-free double layer, which marks the transition between the first and second presheathes, is illustrated by the broken line. The position of the double layer considerably depends on the spatial profile of the particle source ; if the ionization of the neutral gas is strong near the wall, the double layer get near the wall. On the contrary, it move away from the wall if the particle source is localized in the region close to the

center of the plasma.

The ion distribution function at the edge of the second presheath is shown Fig. 7. Due to the formation of the double layer the ion distribution function is separated into two parts. The high energy beam-like part with a small velocity spread is the distribution function of the ions produced in the first presheath and accelerated by the double layer potential, and a low energy part is one of the ions produced in the second presheath. The particle density of the cold ions is smaller than a tenth of that of the energetic ions at the second presheath.

The potential profile in the double layer is numerically calculated from Eq. (12). We obtain the plots in Fig. 8, where the Debye length is defined using the cold ion temperature T_c and the particle density at $x = 0$. The potential changes gradually over the double layer, width of which is about fifty times as large as the Debye length. The corresponding profile of the particle density difference $\delta n \equiv Zn_i - n_e$ illustrated in Fig. 9 shows that two equal but opposite space-charge layers create the localized electrostatic potential structure. While the cold electrons are reflected by the double layer potential, many particle of the hot electrons can reach the second presheath beyond the double layer potential. The ions produced in the first presheath are accelerated toward the wall by the double layer potential. In the first stage of the double layer, the space charge becomes positive due to the reflection of the cold electrons, and it changes to negative in the second stage due to acceleration of the ions and existence of the hot electrons. Discontinuous change of the space charge at $x \simeq x_D + 20\lambda_{d0}$ is due to existence of a small number of the cold ions produced in the second presheath which are reflected by

the double layer and can't move in the layer. It is seen from the fact mentioned above that the double layer structure is composed of four species, that is, the cold electrons, the hot electrons, the energetic ions accelerated by the double layer, and a small number of the cold ions produced in the second presheath.

A double-layer solution without current of the Vlasov-Poisson equations has previously been found by Perkins et al.[18], but, the double layer described in the present paper is different from theirs in the presence of particle flux ; a currentless solution in their analysis is found by symmetrizing the velocity distribution of the plasma, so that the solution involves no mass flow. Recently, Hairapetian et al.[9] have observed a stationary, current-free, double layer in a two-electron-population plasma, which is formed due to self-consistent separation of two electron species. The double layer in their experiment is surrounded by the monotonically decreasing presheath potentials, and the potential drop at the double layer is of the order of the "effective" temperature of energetic electrons. This double layer is set up at a place far from the end plate because ionization and charge-exchange collisions are restricted to the vicinity of the gas valve located at the opposite side of the end plate. Although cold ions were not observed at downstream of the double layer, the formation mechanism and the characteristics described in their paper agree well with those presented in this paper.

V. CONCLUSIONS

We theoretically have investigated the formation of an electrostatic potential due to ionization of neutral atoms in a two-electron-temperature plasma. The plasma equation is analytically solved to show the possibility of steady-state potential formation, and to evaluate the potential drop in such a plasma.

The potential drop in the plasma is continuously changing with increase of the hot- to total electron density ratio if the hot- to cold electron temperature ratio is small. It, however, is allowed to have either a small value characterized by the cold electrons or a large one by the hot electrons if the temperature ratio is greater than ten, and discontinuously changes from the small value to the large one at a critical value for the hot- to total electron density ratio. It is found that a monotonically decreasing potential structure composed by the first presheath, a current-free double layer, the second presheath, and the sheath just in front of the wall can be steadily formed in a lower range of the density ratio around the critical value. The double layer is formed due to self-consistent separation of two electron species with different temperatures and generation of cold ions at the presheathes. The formation mechanism of the present current-free double layer seems to be the same as that of the double layer recently observed in the laboratory experiment[9]. The double layer marks the transition between the first and second presheathes with different potential levels. The position of the double layer is altered by changing the spatial profile of the particle source, and its amplitude depends on the relative density and temperature of two electron species.

ACKNOWLEDGEMENT

We are happy to thank Yukio Ishikawa and Yoshiki Ikeda for their assistance in numerical calculations. This work is partly supported by the cooperation program in the National Institute for Fusion Science in Japan.

REFERENCES

[1]B. Lipschultz, B. LaBombard, H. L. Manning, J. L. Terry, S. Knowlton, E. S. Marmar, M. Porkolab, J. Rice, Y. Takase, S. Texter, and A. Wan, Nucl. Fusion **26**, 1463 (1986).

[2]S. Takamura, A. Sato, Y.Shen, and T. Okuda, J. Nucl. Mater. **149**, 212 (1987).

[3]K. Kurihara, T. Saito, Y. Kiwamoto, and S. Miyoshi, J. Phys. Soc. of Japan **58**, 3453 (1989).

[4]O. Fukumasa, J. Phys. D: Appl. Phys. **22**, 1668 (1989).

[5]E. K. Storm, H. G. Ahlstrom, M. J. Boyle, D. E. Campbell, L. W. Coleman, S. S. Glaros, H. N. Kornblum, R. A. Lerche, D. R. MacQuigg, D. W. Phillion, F. Rainer, R. Rienecker, V. C. Rupert, V. W. Slivinsky, D. R. Speck, C. D. Swift, and K. G. Tirsell, Phys. Rev. Lett. **40**, 1570 (1978).

[6]B. Bezzerides, D. W. Forslund, and E. L. Lindman, Phys. Fluids **21**, 2179 (1978).

[7]L. M. Wickens, J. E. Allen, and P. T. Rumsby, Phys. Rev. Lett. **41**, 243 (1978).

[8]G. Hairapetian and R. L. Stenzel, Phys. Rev. Lett. **61**, 1607 (1988).

[9]G. Hairapetian and R. L. Stenzel, Phys. Rev. Lett. **65**, 175 (1990).

[10]L. Tonks and I. Langmuir, Phys. Rev. **34**, 876 (1929).

[11]E. R. Harrison and W. B. Thompson, Proc. Phys. Soc. London **74**, 145 (1959).

[12]G. A. Emmert, R. Wieland, A. Mense, and J. Davidson, Phys. Fluids **23**, 803 (1980).

[13]K. Sato, F. Miyawaki, and W. Fukui, Phys. Fluids B **1**, 725 (1989).

[14]For a review of laboratory experiments see the following paper : N. Sato, in *Proceedings of the Symposium on Plasma Double Layers* (Roskilde, Denmark, 1982), p.116 ; N. Hershkowitz, Space Sci. Rev. **41**, 351 (1985).

[15]L. P. Block, Astrophys. Space Sci. **55**, 59 (1978).

[16]C. E. Pearson, *Handbook of Applied Mathematics* (Van Nostrand Reinhold, New York, 1983), p.603.

[17]K. U. Riemann, Phys. Fluids B **1**, 961 (1989).

[18]F. W. Perkins and Y. C. Sun, Phys. Rev. Lett. **46**, 115 (1981).

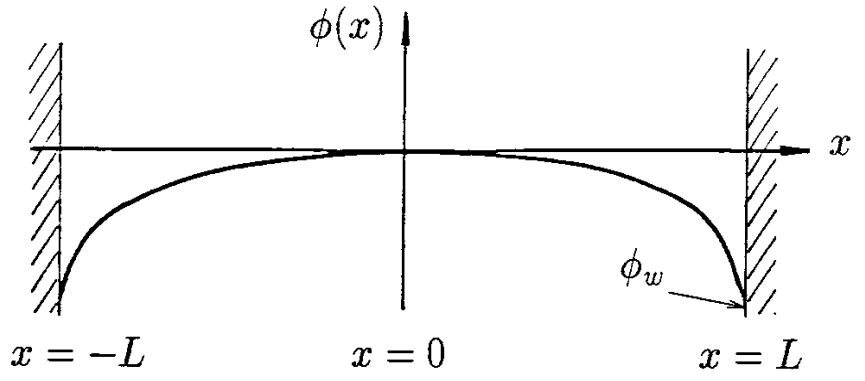

Fig. 1 A schematic diagram of the geometry of the problem.

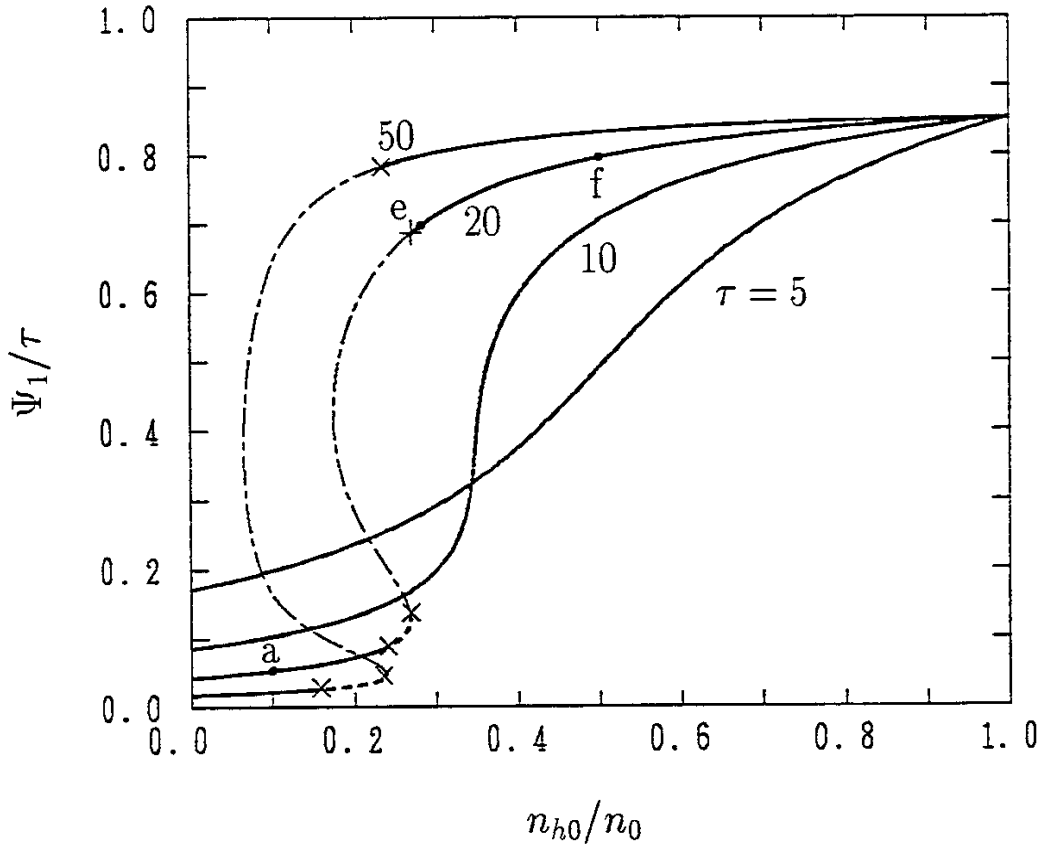

Fig. 2 The normalized potential (solid lines) at the plasma-sheath boundary as a function of the hot- to total density ratio n_{h0}/n_0 for various values of the temperature ratio, $\tau \equiv T_h/T_c$. The broken lines show the solution of Eq. (7) which doesn't satisfy a condition for the sheath formation expressed by the inequality (15).

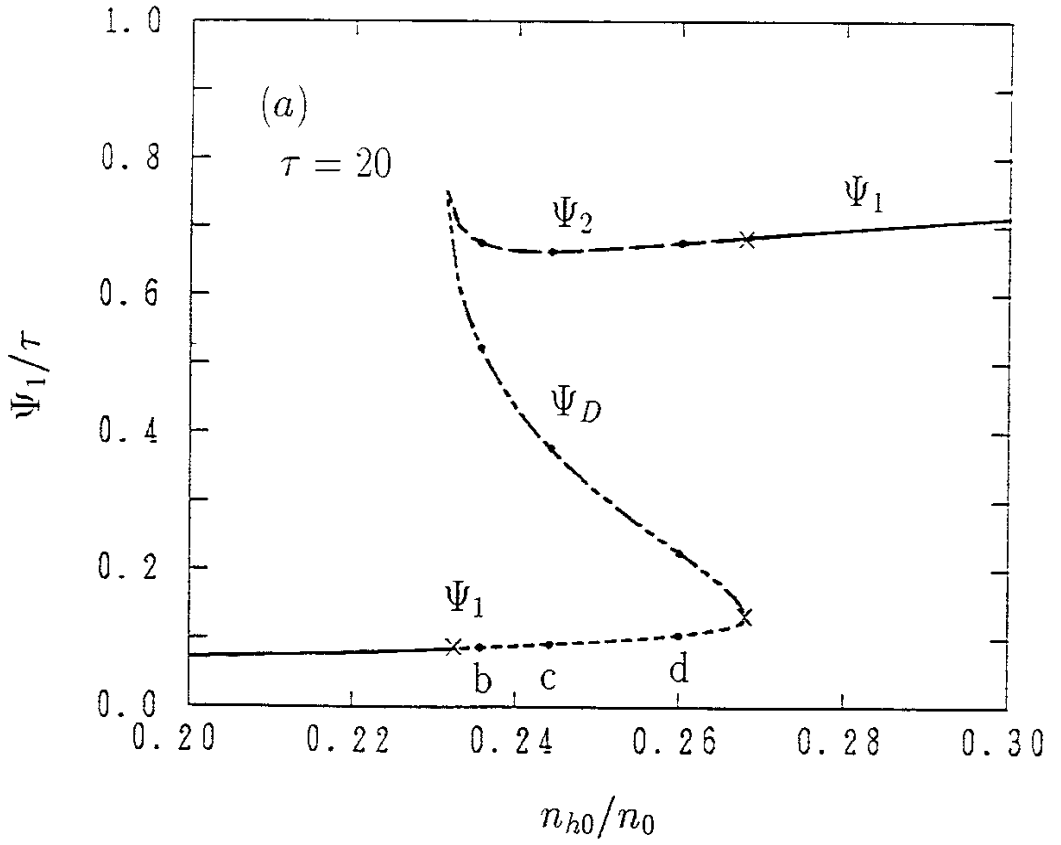

Fig. 3(a) The normalized potentials at the edge of the first presheath, Ψ_1, at the edge of the double layer, Ψ_D, and at the edge of the second presheath, Ψ_2, as a function of the density ratio n_{h0}/n_0 for $\tau = 20$.

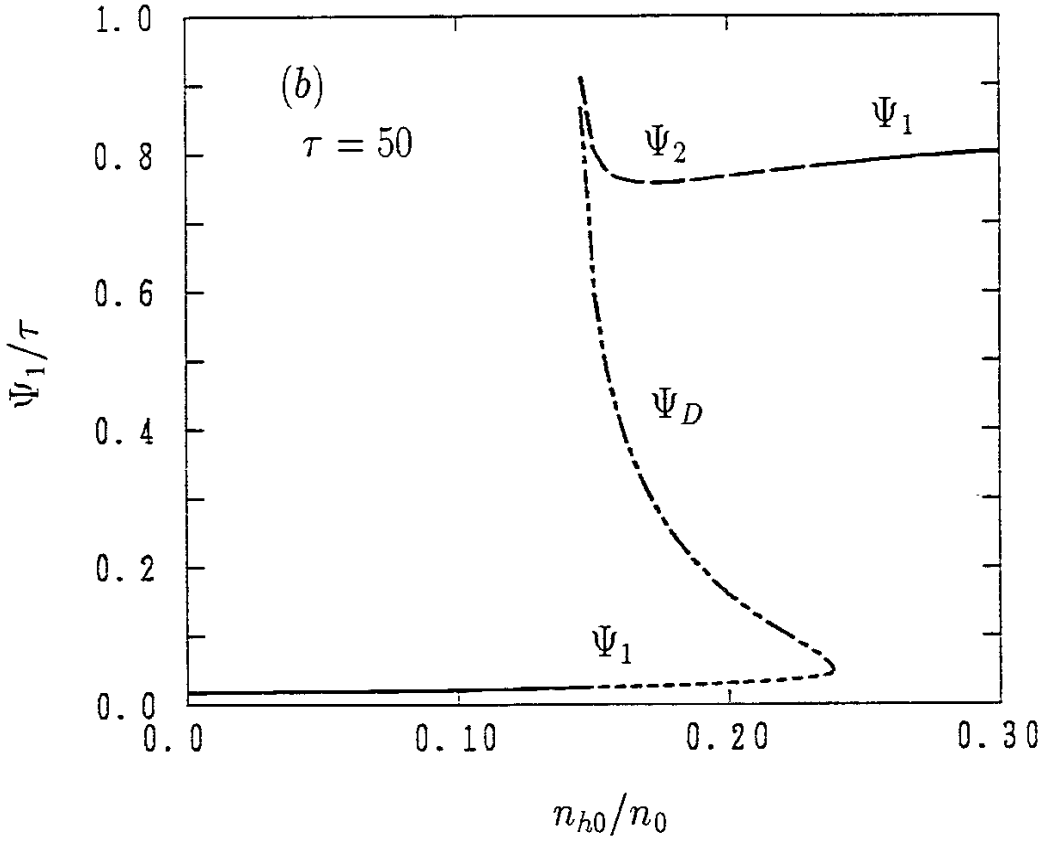

Fig. 3(b) The normalized potentials at the edge of the first presheath, Ψ_1, at the edge of the double layer, Ψ_D, and at the edge of the second presheath, Ψ_2, as a function of the density ratio n_{h0}/n_0 for $\tau = 50$.

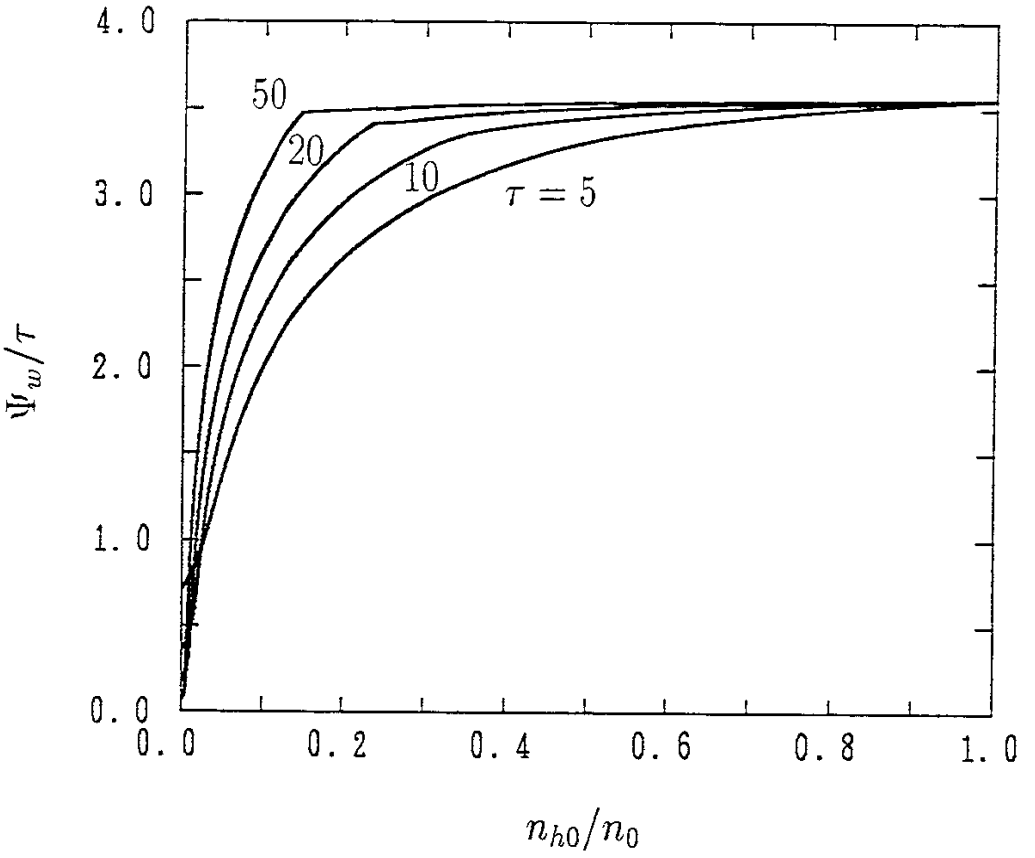

Fig. 4 The normalized wall potential as a function of the density ratio for a hydrogen plasma with various values of the temperature ratio.

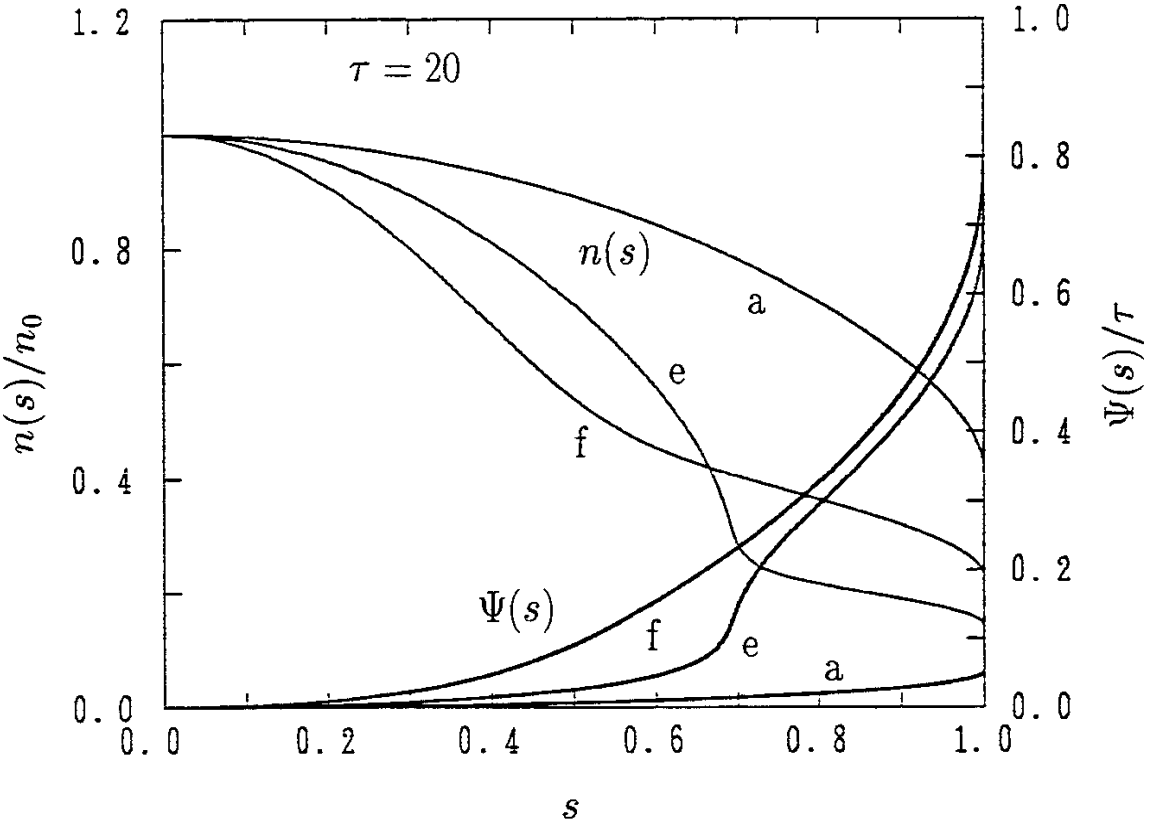

Fig. 5 Profiles of the normalized presheath potential (thick lines) and the particle density (thin lines) for $n_{h0}/n_0 = 0.10$, 0.28, and 0.50, where the spatial profile of the particle source is chosen as $h(s) = n(s)/n_0$. The wall is located at $s = 1$. Symbols a, e, and f represent results for the points in Fig. 2.

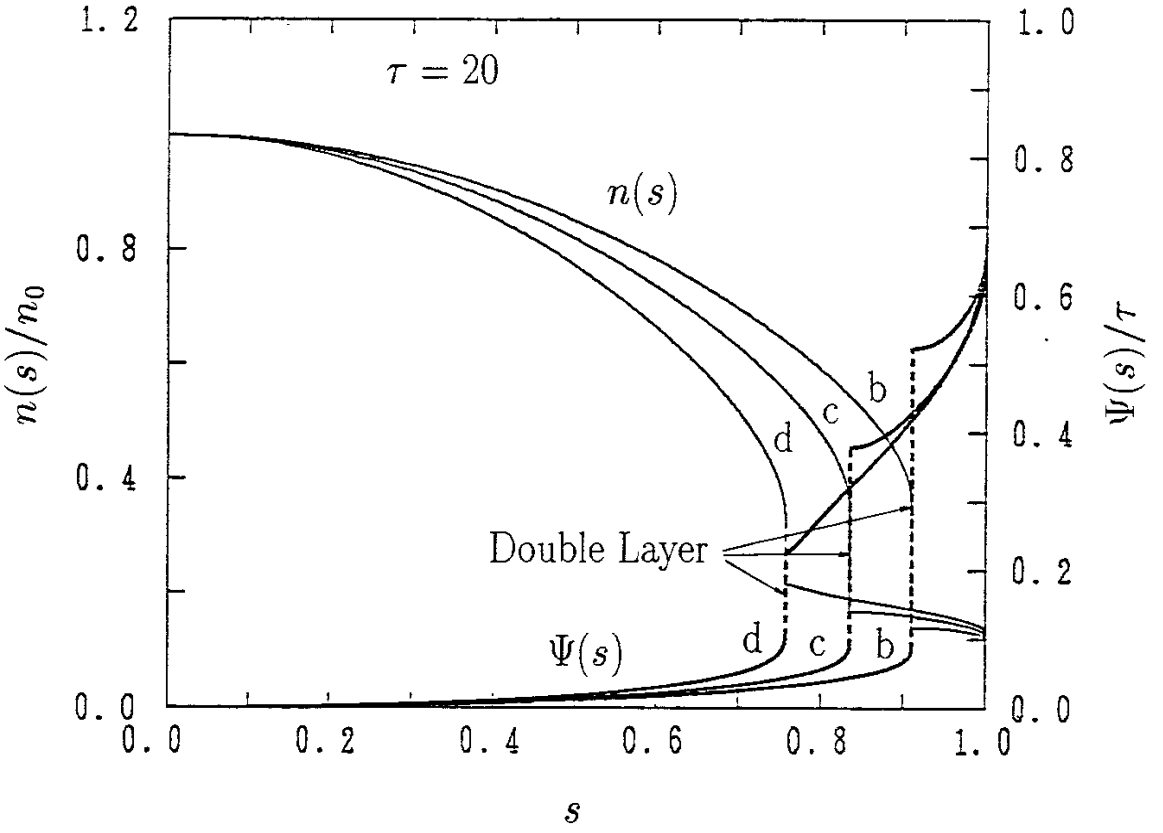

Fig. 6 Profiles of the normalized presheath potential (thick lines) and the particle density (thin lines) for $n_{h0}/n_0 = 0.234$, 0.244, and 0.260, where the spatial profile of the particle source is chosen as $h(s) = n(s)/n_0$. The broken lines show the potential drop at the double layer. The results for the points in Fig. 3(a) are marked with symbols b, c, and d.

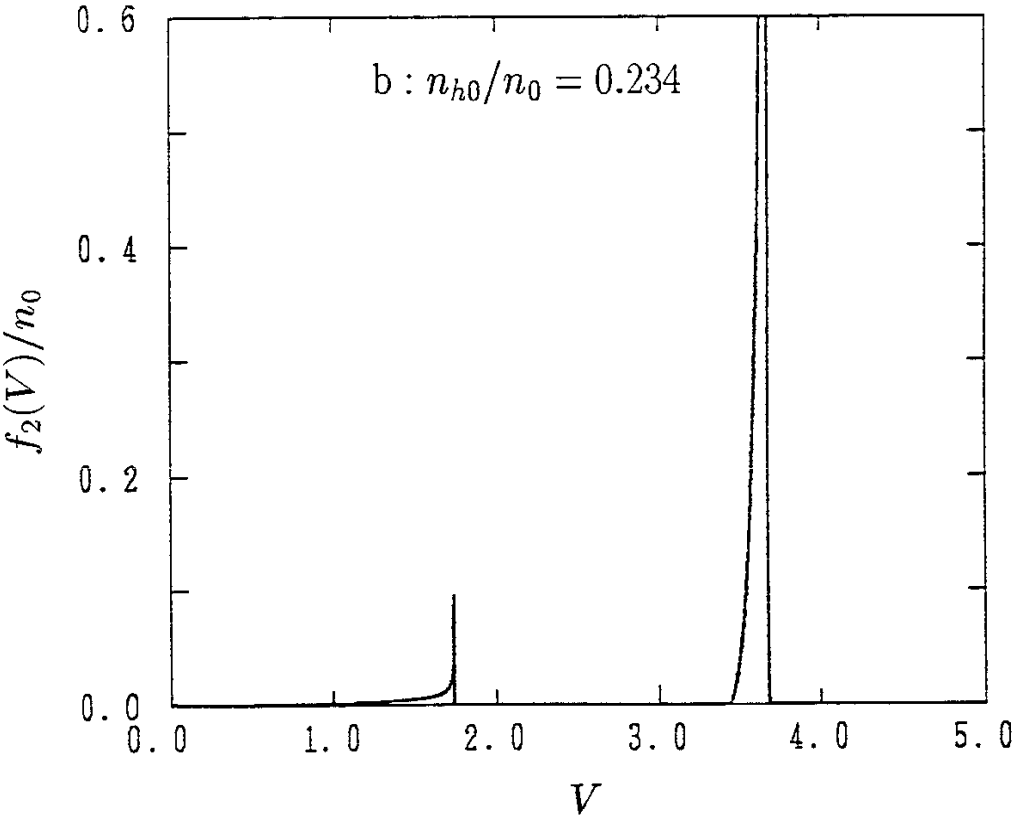

Fig. 7 The normalized ion distribution function at the edge of the second presheath for $Z = 1$, $\tau = 20$, and $n_{h0}/n_0 = 0.234$, where the velocity is normalized as $V = v/(2kT_e/M)^{1/2}$.

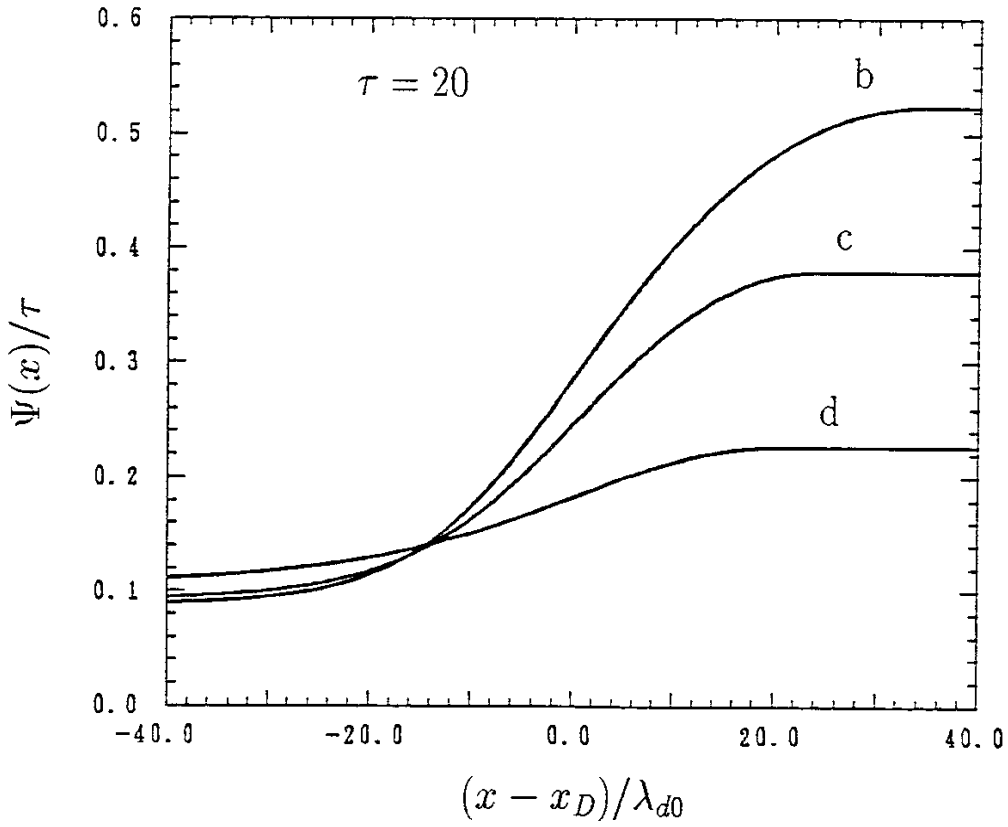

Fig. 8 The profile of the normalized potential at the double layer, where x_D is the position determined from $Zn_i = n_e$. The Debye length is defined using the particle density at $x = 0$ and the cold electron temperature T_c.

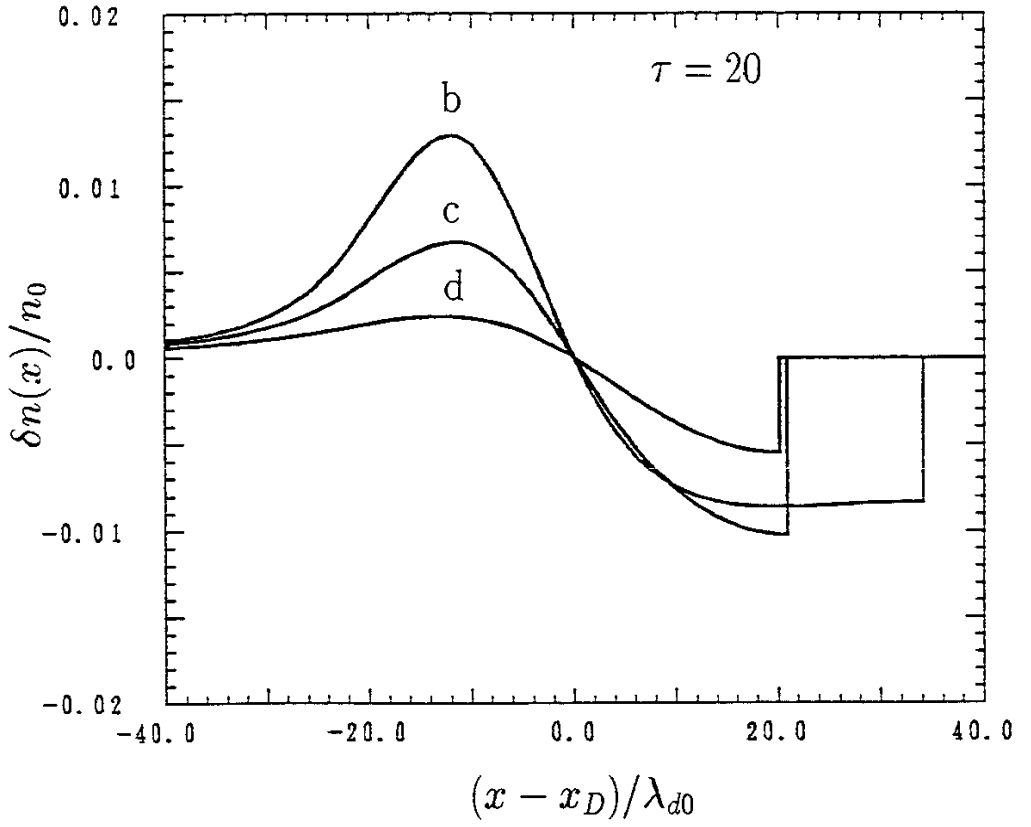

Fig. 9 The profile of the density difference $\delta n \equiv Zn_i - n_e$ at the double layer.

Recent Issues of NIFS Series

NIFS-73 Y.Nomura, Yoshi.H.Ichikawa and W.Horton, *Stabilities of Regular Motion in the Relativistic Standard Map*; Feb. 1991

NIFS-74 T.Yamagishi, *Electrostatic Drift Mode in Toroidal Plasma with Minority Energetic Particles,* Feb. 1991

NIFS-75 T.Yamagishi, *Effect of Energetic Particle Distribution on Bounce Resonance Excitation of the Ideal Ballooning Mode,* Feb. 1991

NIFS-76 T.Hayashi, A.Tadei, N.Ohyabu and T.Sato, *Suppression of Magnetic Surface Breading by Simple Extra Coils in Finite Beta Equilibrium of Helical System;* Feb. 1991

NIFS-77 N. Ohyabu, *High Temperature Divertor Plasma Operation*; Feb. 1991

NIFS-78 K.Kusano, T. Tamano and T. Sato, *Simulation Study of Toroidal Phase-Locking Mechanism in Reversed-Field Pinch Plasma*; Feb. 1991

NIFS-79 K. Nagasaki, K. Itoh and S. -I. Itoh, *Model of Divertor Biasing and Control of Scrape-off Layer and Divertor Plasmas*; Feb. 1991

NIFS-80 K. Nagasaki and K. Itoh, *Decay Process of a Magnetic Island by Forced Reconnection*; Mar. 1991

NIFS-81 K. Takahata, N. Yanagi, T. Mito, J. Yamamoto, O.Motojima and LHDDesign Group, K. Nakamoto, S. Mizukami, K. Kitamura, Y. Wachi, H. Shinohara, K. Yamamoto, M. Shibui, T. Uchida and K. Nakayama, *Design and Fabrication of Forced-Flow Coils as R&D Program for Large Helical Device*; Mar. 1991

NIFS-82 T. Aoki and T. Yabe, *Multi-dimensional Cubic Interpolation for ICF Hydrodynamics Simulation*; Apr. 1991

NIFS-83 K. Ida, S.-I. Itoh, K. Itoh, S. Hidekuma, Y. Miura, H. Kawashima, M. Mori, T. Matsuda, N. Suzuki, H. Tamai, T.Yamauchi and JFT-2M Group, *Density Peaking in the JFT-2M Tokamak Plasma with Counter Neutral Beam Injection* ; May 1991

NIFS-84 A. Iiyoshi, *Development of the Stellarator/Heliotron Research*; May 1991

NIFS-85 Y. Okabe, M. Sasao, H. Yamaoka, M. Wada and J. Fujita, *Dependence of Au^- Production upon the Target Work Function in a Plasma-Sputter-Type Negative Ion Source;* May 1991

NIFS-86 N. Nakajima and M. Okamoto, *Geometrical Effects of the Magnetic Field on the Neoclassical Flow, Current and Rotation in General Toroidal Systems*; May 1991

NIFS-87 S. -I. Itoh, K. Itoh, A. Fukuyama, Y. Miura and JFT-2M Group, *ELMy-H mode as Limit Cycle and Chaotic Oscillations in Tokamak Plasmas;* May 1991

NIFS-88 N.Matsunami and K.Kitoh, *High Resolution Spectroscopy of H^+ Energy Loss in Thin Carbon Film;* May 1991

NIFS-89 H. Sugama, N. Nakajima and M.Wakatani, *Nonlinear Behavior of Multiple-Helicity Resistive Interchange Modes near Marginally Stable States;* May 1991

NIFS-90 H. Hojo and T.Hatori, *Radial Transport Induced by Rotating RF Fields and Breakdown of Intrinsic Ambipolarity in a Magnetic Mirror*; May 1991

NIFS-91 M. Tanaka, S. Murakami, H. Takamaru and T.Sato, *Macroscale Implicit, Electromagnetic Particle Simulation of Inhomogeneous and Magnetized Plasmas in Multi-Dimensions;* May 1991

NIFS-92 S. - I. Itoh, *H-mode Physics, -Experimental Observations and Model Theories-, Lecture Notes, Spring College on Plasma Physics, May 27 - June 21 1991 at International Centre for Theoretical Physics (IAEA UNESCO) Trieste, Italy ;* Jun. 1991

NIFS-93 Y. Miura, K. Itoh, S. - I. Itoh, T. Takizuka, H. Tamai, T. Matsuda, N. Suzuki, M. Mori, H. Maeda and O. Kardaun, *Geometric Dependence of the Scaling Law on the Energy Confinement Time in H-mode Discharges;* Jun. 1991

NIFS-94 H. Sanuki, K. Itoh, K. Ida and S. - I. Itoh, *On Radial Electric Field Structure in CHS Torsatron / Heliotron;* Jun. 1991

NIFS-95 K. Itoh, H. Sanuki and S. - I. Itoh, *Influence of Fast Ion Loss on Radial Electric Field in Wendelstein VII-A Stellarator;* Jun. 1991

NIFS-96 S. - I. Itoh, K. Itoh, A. Fukuyama, *ELMy-H mode as Limit Cycle and Chaotic Oscillations in Tokamak Plasmas;* Jun. 1991

NIFS-97 K. Itoh, S. - I. Itoh, H. Sanuki, A. Fukuyama, *An H-mode-Like Bifurcation in Core Plasma of Stellarators;* Jun. 1991

NIFS-98 H. Hojo, T. Watanabe, M. Inutake, M. Ichimura and S. Miyoshi, *Axial Pressure Profile Effects on Flute Interchange Stability in the Tandem Mirror GAMMA 10;* Jun. 1991

NIFS-99 A. Usadi, A. Kageyama, K. Watanabe and T. Sato, *A Global Simulation of the Magnetosphere with a Long Tail : Southward and Northward IMF;* Jun. 1991

NIFS-100 H. Hojo, T. Ogawa and M. Kono, *Fluid Description of Ponderomotive Force Compatible with the Kinetic One in a Warm Plasma* ; July 1991

NIFS-101 H. Momota, A. Ishida, Y. Kohzaki, G. H. Miley, S. Ohi, M. Ohnishi K. Yoshikawa, K. Sato, L. C. Steinhauer, Y. Tomita and M. Tuszewski

Conceptual Design of D-^{3}He FRC Reactor "ARTEMIS" ; July 1991

NIFS-102 N. Nakajima and M. Okamoto, *Rotations of Bulk Ions and Impurities in Non-Axisymmetric Toroidal Systems* ; July 1991

NIFS-103 A. J. Lichtenberg, K. Itoh, S. - I. Itoh and A. Fukuyama, *The Role of Stochasticity in Sawtooth Oscillation* ; Aug. 1991

NIFS-104 K. Yamazaki and T. Amano, *Plasma Transport Simulation Modeling for Helical Confinement Systems;* Aug. 1991

NIFS-105 T. Sato, T. Hayashi, K. Watanabe, R. Horiuchi, M. Tanaka, N. Sawairi and K. Kusano, *Role of Compressibility on Driven Magnetic Reconnection ;* Aug. 1991

NIFS-106 Qian Wen - Jia, Duan Yun - Bo, Wang Rong - Long and H. Narumi, *Electron Impact Excitation of Positive Ions - Partial Wave Approach in Coulomb - Eikonal Approximation* ; Sep. 1991

NIFS-107 S. Murakami and T. Sato, *Macroscale Particle Simulation of Externally Driven Magnetic Reconnection;* Sep. 1991

NIFS-108 Y. Ogawa, T. Amano, N. Nakajima, Y. Ohyabu, K. Yamazaki, S. P. Hirshman, W. I. van Rij and K. C. Shaing, *Neoclassical Transport Analysis in the Banana Regime on Large Helical Device (LHD) with the DKES Code;* Sep. 1991

NIFS-109 Y. Kondoh, *Thought Analysis on Relaxation and General Principle to Find Relaxed State;* Sep. 1991

NIFS-110 H. Yamada, K. Ida, H. Iguchi, K. Hanatani, S. Morita, O. Kaneko, H. C. Howe, S. P. Hirshman, D. K. Lee, H. Arimoto, M. Hosokawa, H. Idei, S. Kubo, K. Matsuoka, K. Nishimura, S. Okamura, Y. Takeiri, Y. Takita and C. Takahashi, *Shafranov Shift in Low-Aspect-Ratio Heliotron / Torsatron CHS* ; Sep 1991

NIFS-111 R. Horiuchi, M. Uchida and T. Sato, *Simulation Study of Stepwise Relaxation in a Spheromak Plasma ;* Oct. 1991

NIFS-112 M. Sasao, Y. Okabe, A. Fujisawa, H. Iguchi, J. Fujita, H. Yamaoka and M. Wada, *Development of Negative Heavy Ion Sources for Plasma Potential Measurement* ; Oct. 1991

NIFS-113 S. Kawata and H. Nakashima, *Tritium Content of a DT Pellet in Inertial Confinement Fusion* ; Oct. 1991

NIFS-114 M. Okamoto, N. Nakajima and H. Sugama, *Plasma Parameter Estimations for the Large Helical Device Based on the Gyro-Reduced Bohm Scaling* ; Oct. 1991

NIFS-115 Y. Okabe, *Study of Au^- Production in a Plasma-Sputter Type Negative Ion Source* ; Oct. 1991

NIFS-116 M. Sakamoto, K. N. Sato, Y. Ogawa, K. Kawahata, S. Hirokura, S. Okajima, K. Adati, Y. Hamada, S. Hidekuma, K. Ida, Y. Kawasumi,

M. Kojima, K. Masai, S. Morita, H. Takahashi, Y. Taniguchi, K. Toi and T. Tsuzuki, *Fast Cooling Phenomena with Ice Pellet Injection in the JIPP T-IIU Tokamak;* Oct. 1991

NIFS-117 K. Itoh, H. Sanuki and S. -I. Itoh, *Fast Ion Loss and Radial Electric Field in Wendelstein VII-Λ Stellarator*; Oct. 1991

NIFS-118 Y. Kondoh and Y. Hosaka, *Kernel Optimum Nearly-analytical Discretization (KOND) Method Applied to Parabolic Equations <<KOND-P Scheme>>;* Nov. 1991

NIFS-119 T. Yabe and T. Ishikawa, *Two- and Three-Dimensional Simulation Code for Radiation-Hydrodynamics in ICF*; Nov. 1991

NIFS-120 S. Kawata, M. Shiromoto and T. Teramoto, *Density-Carrying Particle Method for Fluid* ; Nov. 1991

NIFS-121 T. Ishikawa, P. Y. Wang, K. Wakui and T. Yabe, *A Method for the High-speed Generation of Random Numbers with Arbitrary Distributions;* Nov. 1991

NIFS-122 K. Yamazaki, H. Kaneko, Y. Taniguchi, O. Motojima and LHD Design *Group, Status of LHD Control System Design ; Dec. 1991*

NIFS-123 Y. Kondoh, *Relaxed State of Energy in Incompressible Fluid and Incompressible MHD Fluid* ; Dec. 1991

NIFS-124 K. Ida, S. Hidekuma, M. Kojima, Y. Miura, S. Tsuji, K. Hoshino, M. Mori, N. Suzuki, T. Yamauchi and JFT-2M Group, *Edge Poloidal Rotation Profiles of H-Mode Plasmas in the JFT-2M Tokamak ;* Dec. 1991

NIFS-125 H. Sugama and M. Wakatani, *Statistical Analysis of Anomalous Transport in Resistive Interchange Turbulence* ;Dec. 1991

NIFS-126 K. Narihara, *A Steady State Tokamak Operation by Use of Magnetic Monopoles* ; Dec. 1991

NIFS-127 K. Itoh, S. -I. Itoh and A. Fukuyama, *Energy Transport in the Steady State Plasma Sustained by DC Helicity Current Drive* ;Jan. 1992

NIFS-128 Y. Hamada, Y. Kawasumi, K. Masai, H. Iguchi, A. Fujisawa, JIPP T-IIU Group and Y. Abe, *New High Voltage Parallel Plate Analyzer* ; Jan. 1992

NIFS-129 K. Ida and T. Kato, *Line-Emission Cross Sections for the Charge-exchange Reaction between Fully Stripped Carbon and Atomic Hydrogen in Tokamak Plasma*; Jan. 1992

NIFS-130 T. Hayashi, A. Takei and T. Sato, *Magnetic Surface Breaking in 3D MHD Equilibria of l=2 Heliotron* ; Jan. 1992

NIFS-131 K. Itoh, K. Ichiguchi and S. -I. Itoh, *Beta Limit of Resistive Plasma in Torsatron/Heliotron* ; Feb. 1992